



HAL
open science

Small molecule activation with divalent samarium triflate: a synergistic effort to cleave O₂

Mathieu Xemard, Marie Cordier, Elisa Louyriac, Laurent Maron, Carine Clavaguera, Grégory Nocton

► To cite this version:

Mathieu Xemard, Marie Cordier, Elisa Louyriac, Laurent Maron, Carine Clavaguera, et al.. Small molecule activation with divalent samarium triflate: a synergistic effort to cleave O₂. Dalton Transactions, 2018, 47 (28), pp.9226-9230. 10.1039/c8dt02196a . hal-01999446

HAL Id: hal-01999446

<https://hal.science/hal-01999446>

Submitted on 11 Nov 2020

HAL is a multi-disciplinary open access archive for the deposit and dissemination of scientific research documents, whether they are published or not. The documents may come from teaching and research institutions in France or abroad, or from public or private research centers.

L'archive ouverte pluridisciplinaire **HAL**, est destinée au dépôt et à la diffusion de documents scientifiques de niveau recherche, publiés ou non, émanant des établissements d'enseignement et de recherche français ou étrangers, des laboratoires publics ou privés.



Small molecules activation with divalent samarium triflate: a synergistic effort to cleave O₂

Received 00th January 20xx,
Accepted 00th January 20xx

Mathieu Xémard,^a Marie Cordier,^a Elisa Louyriac,^b Laurent Maron,^b Carine Clavaquera*^c and Grégory Nocton*^a

DOI: 10.1039/x0xx00000x

www.rsc.org/

The divalent samarium triflate salt does not react with CO₂ or water but does with traces O₂ or N₂O to form a tetrameric bis-oxo samarium motif. The reaction with O₂ is a 4e-reductive cleavage whose electrons are coming from four different samarium centers. This highlights a rare synergistic effect to cleave O₂, which has no precedent with divalent lanthanides complexes. Additionally, the addition of CO₂ on the tetrameric bis-oxo intermediate leads to the formation of a tetrameric bis-carbonate samarium triflate. Thus, the concomitant reaction of CO₂ with traces of O₂ leads to the same bis-carbonate tetrameric assembly.

The chemistry of low-valent coordination compounds has multiple assets in which the small molecules activation is prominent because of the growing importance of transforming abundant, such as N₂, H₂O and O₂,¹⁻⁶ and/or pollutant molecules, such as N₂O,⁷ NO,⁸ CO,^{9, 10} and CO₂,¹¹ at low economical and environmental cost. In this context, electron rich transition metals complexes or low-valent uranium are often used since they allow multiple electron-transfer steps leading to the complete reductive cleavage of the considered small molecule.¹²⁻¹⁷

On the other hand divalent lanthanides do not allow multiple electron transfers^{4, 6, 18, 19} since the trivalent form is the most stable one, except for Ce^{III} that is easily oxidized to formal Ce^{IV}.^{5, 6, 20-24} However, once the single electron transfer step has occurred, the development of a radical on the small molecule often leads to further reactivity, either radical-coupling reactions^{25, 26} or the formation of dianionic species by combination of the radical intermediate with a second coordination metal compound.²⁷ The synergy between two

metallic fragments provides two electrons for the reduction of the substrate and the reaction with N₂O forms oxo dimers,⁷ while the reaction with CO₂ leads to oxalate or carbonate species depending upon various factors.^{11, 28-30}

The mechanism of the carbonate formation is particularly interesting since it involves a bent CO₂²⁻ fragment, formed in between two lanthanide metal centers, which further reacts with another CO₂ yielding CO and CO₃²⁻.³¹ The overall reaction is a two-electron disproportionation of CO₂ and has the important drawback of releasing CO, also a pollutant. In a recent report, we have detailed the reaction of bulky samarium complexes with CO₂ forming carbonate species.³⁰ In this precedent work, the use of a low quality CO allowed the serendipitous formation of a rare peroxy samarium dimer from the reaction with traces of oxygen.³⁰ In an opposite strategy to the typical one, for which the bulk increase allows cleaner reactions by kinetic control, we reasoned that the decrease of the bulk of the ligand set on the samarium center would possibly allow the involvement of more than two samarium centers, *i.e.* more than two electrons. The triflate ligand set is particularly interesting in this matter since it is a multidentate ligand³² that usually facilitates the formation of large assemblies.³³

The present work reports the reactivity studies of O₂, CO₂ and N₂O with the Sm^{II}(OTf)₂(dme)₂ complex and highlights the formation of two tetrametallic assemblies of Sm^{III}. The reductive cleavage of O₂ and the formation mechanism of a carbonate containing tetramer will be discussed.

The reaction of a deep purple solution Sm^{II}(OTf)₂(dme)₂ in thf, with one atmosphere of clean CO₂ does not lead to any discolouration and no change in the ¹⁹F NMR. This contrasts with the many other reports in the literature, including ours, which describe a fast reactivity of CO₂ with divalent samarium complexes at room temperature. However, the redox potential of samarium is known to be extremely dependent of the ligand.³⁴ Additionally, the addition of several equivalents of water does not modify the fate of the reactions. However, when CO₂ of lower quality is used or when traces of O₂ are allowed in by the experimental protocol, the purple thf

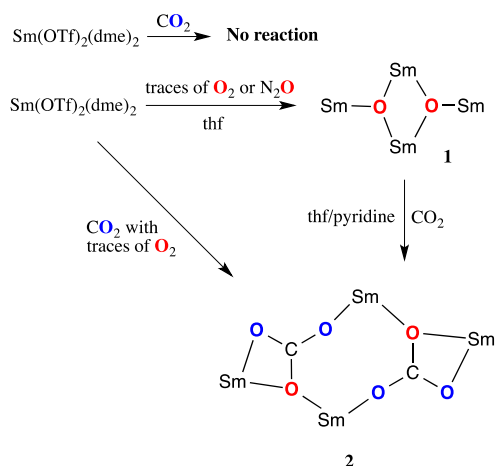
^a LCM, CNRS, Ecole polytechnique, Route de Saclay, 91128 Palaiseau Cedex, France, greg.nocton@polytechnique.edu.

^b LPCNO, UMR 5215, Université de Toulouse-CNRS, INSA, UPS, Toulouse, France

^c Laboratoire de Chimie Physique, CNRS-Université Paris-Sud, Université Paris-Saclay, 15 avenue Jean Perrin, 91405 Orsay Cedex, France, carine.clavaquera@u-psud.fr.

Electronic Supplementary Information (ESI) available: details on synthesis, reactivity studies, ¹⁹F NMR studies, theoretical calculations and X-ray studies. See DOI: 10.1039/x0xx00000x

solution of $\text{Sm}^{\text{II}}(\text{OTf})_2$ slowly fades until it gets clear. After the filtration of the solution, pentane layering allowed the formation of transparent crystals that were analyzed as a tetrameric assembly of samarium containing two carbonate dianion, $[\text{Sm}_4(\mu_3\text{-CO}_3\text{-}\kappa_4\text{O,O'})_2(\mu_2\text{-OTf})_6(\text{OTf})_2\text{Sm}(\text{thf})_{10}]$, (**2**) (Scheme 1). The formation of carbonate dianion from CO_2 with samarium complexes has precedent in the literature and several mechanisms are proposed: i) the oxo formation from CO_2 with CO release and following CO_2 insertion or ii) the reductive disproportionation of two CO_2 with CO release. The key point here is that a clean CO_2 in a rigorous experimental setup does not react with $\text{Sm}^{\text{II}}(\text{OTf})_2(\text{dme})_2$. It means that CO_2 is not the unique reactant in this reaction and the oxo intermediate mechanism should be privileged. Therefore, we started to investigate the formation mechanism of this tetrameric assembly using N_2O but also O_2 , a more challenging way of forming oxo compounds with divalent lanthanides complexes.



Scheme 1. Synthetic scheme for **1** and **2**.

Reacting a degassed deep purple thf solution of $\text{Sm}(\text{OTf})_2(\text{dme})_2$ with N_2O leads to the complete discoloration of the solution in approximately 15 hours and an intractable white precipitate crashes out. Filtration and slow evaporation of the solvents allowed the crystallization of the bis-oxo tetramer $[\text{Sm}_4(\mu_3\text{-O})_2(\mu_2\text{-OTf})_6(\mu_3\text{-OTf})_2(\text{thf})_4(\text{dme})_2]$ (**1**) in good yields (85%) a pure analytical form. On the other hand, the reaction of $\text{Sm}(\text{OTf})_2(\text{dme})_2$ with one atmosphere of dry O_2 in thf is not clean and leads to an intractable clear powder and trivalent samarium triflate.

X-Ray suitable crystals of **1** were grown by slow diffusion of pentane in a thf solution giving access to the topology of the oxo complex (Fig. 1a). It crystallizes in the monoclinic $\text{P2}_1/\text{n}$ space group (Table S1). The $[\text{Sm}_2(\mu_3\text{-O})]_2$ core of the tetramer is composed of four samarium centers bridged by two μ^3 -oxo anions (Fig. 1a). In the asymmetric unit (half of the molecule) one samarium center is 8-coordinated bearing only one coordinated thf molecule while the second one is 8-coordinated and bears one coordinated thf molecule and one dme molecule. The Sm-O distances on the O^{2-} centers are of

2.207(7) Å, 2.258(8) and 2.271(7) Å, which is much longer than the Sm-O distances previously reported on μ_2 -oxo (2.094 Å for the $(\text{Cp}^*_2\text{Sm})_2(\mu\text{-O})$ complex).⁷ However, these are similar than the Sm-O distance observed with the μ_3 -oxo samarium cluster (average distance of 2.211 Å) reported by Hosmane.³⁵ The Sm-O-Sm angles (varying between 101.3(3)° and 133.2(4)°) show an important dissymmetry around the oxo where the Sm-O-Sm angles in Hosmane's cluster are between 118.9(2)° and 119.4(2)°. As expected, the triflate anions are favoring the tetrametallic assembly by bridging between different lanthanide centres (two of them are bringing between two Sm centers whereas the third OTf anion of the asymmetric unit is bridging between three centres). The Sm-O distances are varying between 2.400(8) Å and 2.490(8) Å for μ_2 -OTf and between 2.484(7) Å and 2.596(7) Å for μ_3 -OTf with an average of 2.47(5) Å. These distances are shorter than the one observed on the previously reported divalent $\text{Sm}(\text{OTf})_2$ complexes³⁶ (average of 2.543 Å for $[\text{Sm}(\text{OTf})_2(\text{thf})_{1.5}]_n$), in agreement with the oxidation of the samarium center. The mean Sm-O distance is longer for the μ_3 -OTf anion than for μ_2 -OTf ones (2.52(7) Å vs 2.45(3) Å).

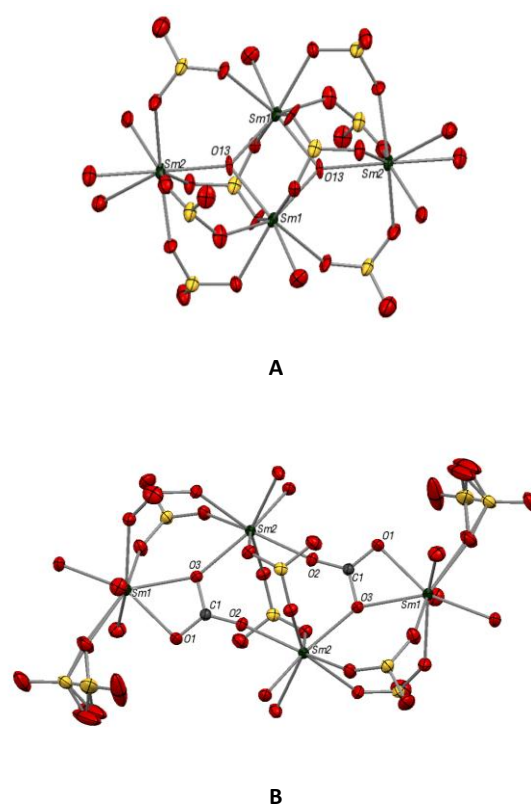


Figure 1. A) ORTEP of **1**; hydrogen, carbon and fluorine atoms are removed for clarity; Sm green, O red, S yellow. Selected distances (Å) and angles (°): SmO1-O13 2.271(7), SmO2-O13 2.207(7), SmO1-O13#3 2.250(8), SmO1-SM01#3 3.497(1), SmO1-SM02#3 3.940(1), SmO1-O13-SmO2 133.2(4), SmO1-O13-SmO1#3 101.3(3), SmO1#3-O13-SmO1 124.2(3). B) ORTEP of **2-thf**; hydrogen, carbon (excepted C1) and fluorine atoms are removed for clarity; Sm green, O red, S yellow. Selected distances (Å) and angles (°): Sm1-Sm2 4.580, Sm1-Sm1#2 10.102, Sm2-Sm2#2 4.522, Sm1-O1 2.379(2), Sm1-O3 2.392(2), Sm2-O2#2 2.295(2), Sm2-O3 2.362(2), O1-C1-O2 125.1(2), O1-C1-O3 115.8(2).

Reacting a thf suspension or a thf/pyridine solution of **1** with CO₂ leads respectively after filtration and layering with pentane to [Sm₄(μ₃-CO₃-κ₄O,O',O'')₂(μ₂-OTf)₆(OTf)₂Sm(thf)₁₀] (**2-thf**) and to [Sm₄(μ₃-CO₃-κ₄O,O',O'')₂(μ₂-OTf)₆(OTf)₂Sm(py)₁₀] (**2-py**) as large colorless crystals (Fig. 1b). The **2-thf** cluster can also be obtained in good yield (80%) by direct reaction of the raw suspension obtained from the reaction of Sm(OTf)₂(dme)₂ with N₂O.

X-Ray diffraction analysis shows that **2-thf** crystallize in a *P*-1 triclinic space-group and **2-py** in a *P*2₁/*n* monoclinic one. For both assemblies, half the molecule is obtained as the image of the other half by an inversion centre and the roughly planar core can be described as [Sm₂(μ₃-η₂(O,O')₂:η₁(O):η₁(O')-CO₃)₂ with four 8-coordinated Sm surrounding two bridging carbonate anions. The carbonate coordination mode is rather unusual but has already been observed with only few lanthanides clusters, mainly Dy cluster, some of them obtained *via* atmospheric fixation of CO₂ in aqueous media, often implying poor control of the geometry of the cluster and long synthetic procedure.³⁷⁻⁴⁰ The C-O distances in the CO₃²⁻ bridges are between 1.263(2) Å and 1.315(2) Å for **2-thf** and 1.264(8) Å and 1.301(8) Å for **2-py** are in the same range as the C-O distances in NaCO₃ (1.29 Å)⁴¹ but here, the asymmetric coordination mode causes a strong variation between the longest C-O bonds bared by the oxygen bridging between two Sm centers and the shortest bonds. This leads to the same disparity of bonding than the one observed by Gardiner in his porphyrinogen samarium carbonate complex (1.317(7) and 1.276(4) Å)²⁸ or the one observed on the [Cp^{tt}₂Sm]₂(μ-CO₃) complex (between 1.15(1) and 1.18(1) Å).³⁰ The carbonate Sm-O distances are similar in both **2-thf** and **2-py** with a relatively short Sm-O distance on the terminally coordinated oxygen (2.295(1) Å on **2-thf** and 2.275(5) Å on **2-py**) whereas the other distances are longer (between 2.373(4) and 2.399(4) Å for **2-thf** and between 2.39(1) and 2.41(1) Å for **2-py**). As for **1**, two types of triflate anions are observed, one terminal triflate ion and μ² bridging ones. The Sm-O distances on μ₂-TfO⁻ are in the same range as the ones in **1** (2.410(2) Å to 2.472(1) Å with an average of 2.45(3) Å for **2-thf** and 2.425(5) to 2.501(5) with an average of 2.46(3) Å for **2-py**). The number of coordinated solvent molecules is also identical in **2-thf** and **2-py** with two molecules on one samarium and three on the other samarium. In solution, coordinated solvent molecules and triflate ligands are known to possibly exchange.³³ Thereby, the concentration thf solution of Sm(OTf)₂(dme)₂ strongly influences the topology of re-crystallized species, and possibly the reactive species. Indeed, from strongly concentrated solution, only the reported polymer of [Sm(OTf)₂(thf)_{1.5}]_n can be recrystallized,³⁶ but on the other hand, from a diluted solution (ca. 10 mmol.L⁻¹), a tetrametallic assembly has also been isolated (Fig. S16, Table S5). The assemblies, [Sm₂(μ₃-OTf)₂(μ₃-OTf)(OTf)(thf)₆]₂ (**3**) is featuring relatively long Sm-O distances on TfO⁻ anions (average of 2.63(8) Å) compared to 2.54 Å for [Sm(OTf)₂(thf)_{1.5}]_n.³⁶ Although the ¹⁹F solution NMR of Sm(OTf)₂(dme)₂ shows only one broad signal at δ = -70.33 ppm, indicating strong exchange, the isolation of **3** as a tetrameric assembly is an insight into the mechanism involved

in the formation of **1**: the topology of the assembly may be prior to the reactivity with N₂O and/or may lead to the formation of **1** by a concerted mechanism. Moreover the strong similarity between **2-thf** and **2-py** is also good evidence that the core of the cluster, once formed, can be retained in solution and that only solvents molecules are exchanging in solution phase. In order to obtain better insight in the dynamics in solution, **2-thf** was recrystallized from a pyridine solution yielding **2-py**, while the fate of the triflate anions in **1** and **2** was monitored by ¹⁹F NMR. For **1**, only one broad signal is observed at δ = -79.43 ppm in thf (Fig. S1), indicating a fast exchange between the two bridging modes on triflates. On the other hand, for **2-thf**, two broad signals are observed on the ¹⁹F NMR in thf (Fig. S2) at δ = -79.20 ppm and δ = -80.19 ppm. These two signals should correspond to the two available coordination modes on triflate anions. The range of chemical shifts observed for both **1** and **2-thf** is close to the chemical shift observed for Sm(OTf)₃ in thf (δ = -79.30 ppm and δ = -80.10 ppm) but are strongly shifted from the one of the Sm(OTf)₂(dme)₂ starting material which is in agreement with triflates anions on Sm^{III} centres.

The formation of **2** from **1** validates the oxo intermediate mechanism and is not surprising considering the recent work from Roesky^{42, 43} and the seminal study of Meyer on uranium bridged oxo complexes.⁴⁴⁻⁴⁶ The reaction of dry air on **1** is not clean but has led to the re-crystallization of **2**, which is indicative of selective CO₂ abstraction from air. Yet, the presence of humidity in air complicates the reactivity, yielding mostly to Sm(OTf)₃. Such a selective atmospheric fixation of CO₂ on lanthanide hydroxo complexes has already been described by Mazzanti.⁴⁷

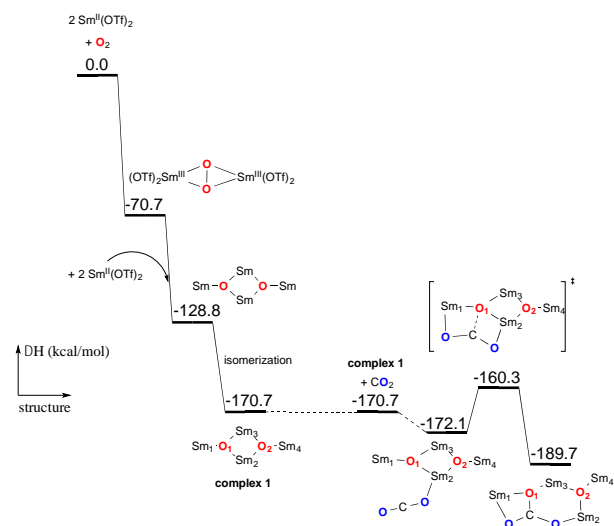


Figure 2. Computed enthalpy profile for the O₂ reductive cleavage by four Sm(OTf)₂ to form **1** and subsequent reaction with CO₂.

Theoretical calculations have been performed on the formation of **1** and **2**. The addition of O₂ between two samarium centers is very favorable in good agreement with our precedent work. The key point here is that the flexibility and low steric bulk of the triflate anions allow the addition of

two more divalent samarium centers to cleave O₂ and form the bis-oxo tetrameric samarium complex **1**. As shown in Figure 2, **1** lies -170.7 kcal/mol below the starting materials, which explains its easy formation. Then, the CO₂ insertion on the bis-oxo complex **1** has been computed and indicates that the transition state is only 11.8 kcal/mol while the reaction is exergonic by 19 kcal/mol (Fig. 2). At the transition state, the CO₂ molecule is strongly activated by two samarium atoms (O-C-O angle around 157°), *i.e.* a double nucleophilic assistance (Sm₁-O₁: 2.60 Å, Sm₂-O₁: 2.55 Å). The oxo group O₁ adopts a pyramidal shape and is lying 0.58 Å above the Sm₁-Sm₂-Sm₃ plane (compared to 0.25 Å in complex **1**). This situation is due to the π_3 -coordination mode of the oxo O₁ that enforces its remaining p lone pair to point out of the plane inducing an out-of-plane attack of CO₂.

Since the reaction of 1 atmosphere of dry O₂ with the Sm^{II}(OTf)₂(dme)₂ complex in thf was not conclusive, low amount of O₂ was used to mimic what may happen when using a lower quality CO₂ (*i.e.* containing traces amounts of O₂). As such, the deep purple thf solution fades slowly and storage of the colorless solution at -35 °C afforded few crystals of **1** (the yield could not be calculated). The ¹⁹F NMR indicates the formation a broad signal at $\delta = -79.81$ ppm, characteristic of **1**. This indicates that the presence of traces of O₂ allows the formation the bis-oxo species from synergistic action of four samarium centers, each providing one electron to cleave O₂. In this example, the low bulk and the dynamics in solution of the triflate anions allow this synergy. This opens new possibilities for small molecules activation with divalent lanthanides, at the opposite of the typical strategy, which consists in increasing the steric bulk for a better stabilization of the divalent lanthanide center. This example also comes as a warning for the quality of the CO₂ and the rigor of the experimental protocol that should be used for these small activation mechanistic studies.

In conclusion, this article reports the reaction of N₂O and O₂ with the Sm(OTf)₂(dme)₂ divalent samarium precursor to yield a rare tetrametallic bis-oxo complex of Sm^{III}. The reaction with O₂ is, to our knowledge, a unique example of synergic four electrons reductive cleavage O₂ with divalent lanthanide complexes. The subsequent reaction of CO₂ on this bis-oxo complex yields the tetrameric bis-carbonate samarium complex from CO₂ insertion in the oxo-bridge. This work shows that the use of less bulky divalent lanthanide complexes opens new routes for small molecules activation using the synergistic effort of multiple metal centers to cleave molecules that need more than 2e⁻ such as O₂, CO or N₂. Further studies are conducted in this direction.

Notes and references

‡ This project was financed by the French National Agency with grant number ANR-15-CE29-0019. We thank CNRS and Ecole polytechnique for funding. MX is grateful to the DGA for funding. LM is member of the Institut Universitaire de France.

1. C. E. Laplaza, M. J. A. Johnson, J. C. Peters, A. L. Odom, E. Kim, C. C. Cummins, G. N. George and I. J. Pickering, *J. Am. Chem. Soc.*, 1996, **118**, 8623-8638.
2. M. W. Kanan and D. G. Nocera, *Science*, 2008, **321**, 1072-1075.
3. W. Zhang, W. Lai and R. Cao, *Chem. Rev.*, 2017, **117**, 3717-3797.
4. F. Jaroschik, A. Momin, F. Nief, X. F. Le Goff, G. B. Deacon and P. C. Junk, *Angew. Chem. Int. Ed.*, 2009, **48**, 1117-1121.
5. H. B. Kagan, *J. Alloys Compd.*, 2006, **408**, 421-426.
6. M. Szostak and D. J. Procter, *Angew. Chem. Int. Ed.*, 2012, **51**, 9238-9256.
7. W. J. Evans, J. W. Grate, I. Bloom, W. E. Hunter and J. L. Atwood, *J. Am. Chem. Soc.*, 1985, **107**, 405-409.
8. C. L. Ford, Y. J. Park, E. M. Matson, Z. Gordon and A. R. Fout, *Science*, 2016, **354**, 741-743.
9. W. J. Evans, J. W. Grate and R. J. Doedens, *J. Am. Chem. Soc.*, 1985, **107**, 1671-1679.
10. W. J. Evans, M. J. Lipp, C. S. Yoo, H. Cynn, J. L. Herberg, R. S. Maxwell and M. F. Nicol, *Chem. Mater.*, 2006, **18**, 2520-2531.
11. W. J. Evans, C. A. Seibel and J. W. Ziller, *Inorg. Chem.*, 1998, **37**, 770-776.
12. A. R. Fox, S. C. Bart, K. Meyer and C. C. Cummins, *Nature*, 2008, **455**, 341-349.
13. M. Falcone, L. Chatelain, R. Scopelliti, I. Živković and M. Mazzanti, *Nature*, 2017, **547**, 332.
14. M. Falcone, C. E. Kefalidis, R. Scopelliti, L. Maron and M. Mazzanti, *Angew. Chem. Int. Ed.*, 2016, **55**, 12290-12294.
15. C. E. Laplaza and C. C. Cummins, *Science*, 1995, **268**, 861-863.
16. M. M. Rodriguez, E. Bill, W. W. Brennessel and P. L. Holland, *Science*, 2011, **334**, 780-783.
17. D. J. Knobloch, E. Lobkovsky and P. J. Chirik, *Nature Chemistry*, 2009, **2**, 30.
18. H. B. Kagan, *Tetrahedron*, 2003, **59**, 10351-10372.
19. W. J. Evans, D. S. Lee, D. B. Rego, J. M. Perotti, S. A. Kozimor, E. K. Moore and J. W. Ziller, *J. Am. Chem. Soc.*, 2004, **126**, 14574-14582.
20. F. Nief, *Dalton Transactions*, 2010, **39**, 6589-6598.
21. J. A. Bogart, C. A. Lippincott, P. J. Carroll, C. H. Booth and E. J. Schelter, *Chem. Eur. J.*, 2015, **21**, 17850-17859.
22. J. R. Levin, T. Cheisson, P. J. Carroll and E. J. Schelter, *Dalton Trans.*, 2016, **45**, 15249-15258.
23. L. A. Solola, A. V. Zabula, W. L. Dorfner, B. C. Manor, P. J. Carroll and E. J. Schelter, *J. Am. Chem. Soc.*, 2016, **138**, 6928-6931.
24. J. A. Bogart, A. J. Lewis, S. A. Medling, N. A. Piro, P. J. Carroll, C. H. Booth and E. J. Schelter, *Inorg. Chem.*, 2013, **52**, 11600-11607.
25. G. Nocton, W. L. Lukens, C. H. Booth, S. S. Rozenel, S. A. Melding, L. Maron and R. A. Andersen, *J. Am. Chem. Soc.*, 2014, **136**, 8626-8641.
26. G. Nocton and L. Ricard, *Chem. Commun.*, 2015, **51**, 3578-3581.
27. W. J. Evans, *J. Alloys Compd.*, 2009, **488**, 493-510.
28. N. W. Davies, A. S. P. Frey, M. G. Gardiner and J. Wang, *Chem. Commun.*, 2006, 4853-4855.
29. J. Andrez, J. Pécaut, P.-A. Bayle and M. Mazzanti, *Angew. Chem. Int. Ed.*, 2014, **53**, 10448-10452.
30. M. Xémard, V. Goudy, A. Braun, M. Tricoire, M. Cordier, L. Ricard, L. Castro, E. Louyriac, C. E. Kefalidis, C. Clavaguéra, L. Maron and G. Nocton, *Organometallics*, 2017, **36**, 4660-4668.
31. L. Castro, S. Labouille, D. R. Kindra, J. W. Ziller, F. Nief, W. J. Evans and L. Maron, *Chem. Eur. J.* 2012, **18**, 7886-7895.
32. M. Xémard, A. Jaoul, M. Cordier, F. Molton, O. Cador, B. Le Guennic, C. Duboc, O. Maury, C. Clavaguéra and G. Nocton, *Angew. Chem. Int. Ed.*, 2017, **56**, 4266-4271.
33. G. Nocton, F. Burdet, J. Pécaut and M. Mazzanti, *Angew. Chem. Int. Ed.*, 2007, **46**, 7574-7578.

34. E. Prasad, B. W. Knettle and R. A. Flowers, *J. Am. Chem. Soc.*, 2002, **124**, 14663-14667.
35. N. S. Hosmane, Y. Wang, A. R. Oki, H. Zhang and J. A. Maguire, *Organometallics*, 1996, **15**, 626-638.
36. K. Mashima, T. Oshiki and K. Tani, *J. Org. Chem.*, 1998, **63**, 7114-7116.
37. A. S. R. Chesman, D. R. Turner, B. Moubaraki, K. S. Murray, G. B. Deacon and S. R. Batten, *Dalton Trans.*, 2012, **41**, 10903-10909.
38. I. A. Gass, B. Moubaraki, S. K. Langley, S. R. Batten and K. S. Murray, *Chem. Commun.*, 2012, **48**, 2089-2091.
39. L.-L. Li, R. Pan, J.-W. Zhao, B.-F. Yang and G.-Y. Yang, *Dalton Trans.*, 2016, **45**, 11958-11967.
40. S. Xue, L. Zhao, Y.-N. Guo, P. Zhang and J. Tang, *Chem. Commun.*, 2012, **48**, 8946-8948.
41. M. Dusek, G. Chapuis, M. Meyer and V. Petricek, *Acta Crystallogr. B*, 2003, **59**, 337-352.
42. C. Schoo, S. V. Klementyeva, M. T. Gamer, S. N. Konchenko and P. W. Roesky, *Chem. Commun.*, 2016, **52**, 6654-6657.
43. E. Louyriac, P. W. Roesky and L. Maron, *Dalton Trans.* 2017, **46**, 7660-7663.
44. O. P. Lam, S. M. Franke, F. W. Heinemann and K. Meyer, *J. Am. Chem. Soc.*, 2012, **134**, 16877-16881.
45. A. C. Schmidt, F. W. Heinemann, C. E. Kefalidis, L. Maron, P. W. Roesky and K. Meyer, *Chem. Eur. J.*, 2014, **20**, 13501-13506.
46. O. P. Lam, S. C. Bart, H. Kameo, F. W. Heinemann and K. Meyer, *Chem. Commun.* 2010, **46**, 3137-3139.
47. L. Natrajan, J. Pecaut and M. Mazzanti, *Dalton Trans.*, 2006, 1002-1005.